ARTICLE

OBC
www.rsc.org/obc

Antitumor benzothiazoles.† Frontier molecular orbital analysis predicts bioactivation of 2-(4-aminophenyl)benzothiazoles to reactive intermediates by cytochrome P4501A1

Sean E. O'Brien, Helen L. Browne, Tracey D. Bradshaw, Andrew D. Westwell, Malcolm F. G. Stevens and Charles A. Laughton *

Cancer Research Laboratories, School of Pharmaceutical Sciences, University of Nottingham, Nottingham, UK NG7 2RD

Received 17th September 2002, Accepted 2nd December 2002
First published as an Advance Article on the web 17th January 2003

The antitumor and metabolic activities of 2-(4-aminophenyl)benzothiazoles and their fluorinated analogues cannot be explained or predicted by conventional chemical means. Their mode of anti-cancer action involves metabolism of the benzothiazoles to an as yet unidentified reactive species. This species then forms DNA adducts which provoke cell death. The electronic structures and possible intermediates of these compounds have been computed quantum mechanically. The counter-intuitive patterns of metabolism can only be explained by considering the active intermediate to be a nitrenium ion. The distribution of the highest occupied molecular orbital for the nitrenium species derived from each fluorinated analogue correlates perfectly with the production, or otherwise, of an exportable metabolite. Further related compounds have been analyzed by this method and the predictions of their metabolism have subsequently been verified experimentally.

Introduction

The serendipitous discovery of the unique antitumor profile of 2-(4-aminophenyl)benzothiazole (**1**) (Fig. 1) arose when it was prepared as an intermediate in a project seeking routes to polyhydroxylated 2-phenylbenzothiazoles which were required for evaluation as potential tyrosine kinase inhibitors.[2] An unusual feature of the activity of **1** against human breast cancer cell lines *in vitro* is the appearance of a characteristic biphasic dose-response relationship: the compound promotes cell death at sub-nanomolar concentrations but an increase in viable cell population occurs in the micromolar range.[3] Derivatives with a methyl (**2**) or halogen group (Cl, Br or I) in the 3′-position (*e.g.* **3**) have a characteristic *in vitro* activity fingerprint in the NCI 60-cell line panel which, using the NCI's COMPARE analysis software,[4] is unlike other known mechanistic classes of chemotherapeutic agents.[3,5,6] 2-(4-Amino-3-methylphenyl)benzothiazole (**2**: DF 203; NSC 674495) was originally selected as the lead compound for preclinical development from this series as it proved to have superior *in vivo* activity over the 3′-halogeno congeners in human tumor xenograft models.[3,5]

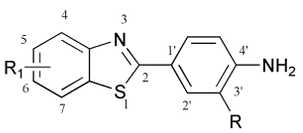

1: R = R_1 = H
2: R = Me, R_1 = H (DF 203; NSC 674495)
3: R = Cl, R_1 = H (NSC 682303)
4: R = Me, R_1 = 6-OH (NSC 703785)
5: R = Me, R_1 = 4-F (4-F 203; NSC 706705)
6: R = Me, R_1 = 5-F (5-F 203; NSC 703786)
7: R = Me, R_1 = 6-F (6-F 203; NSC 702156)
8: R = Me, R_1 = 7-F (7-F 203; NSC 711670)
9: R = Me, R_1 = 5,6-di-F (NSC 711671)
10: R = Me, R_1 = 4,5-di-F
11: R = Me, R_1 = 5,7-di-F
12: R = Cl, R_1 = 5-F (NSC 709927)

Fig. 1 Chemical structures, nomenclature and numbering scheme of bioactive 2-(4-aminophenyl)benzothiazoles.

Subsequently however, metabolic studies demonstrated that **2** was biotransformed to a 6-hydroxy metabolite (**4**) which had no antitumor activity[7] and reversibly inactivated the bioactivating enzyme, cytochrome P450 (CYP) 1A1.[8] Also, compound **2** (or, more likely, a reactive intermediate derived thereof) binds covalently to CYP1A1 microsomes.[8] Furthermore, in conditions sub-maximal for growth, **4** is capable of eliciting a mitogenic response at concentrations between 300 nM and 3 μM in the MCF-7 human breast tumor cell line.[9] We hypothesize that the antagonistic properties of metabolite (**4**) may be responsible for the biphasic response observed in *in vitro* studies. As levels of metabolite (**4**) rise, cell growth resumes, and hence chemical strategies to block the formation of this metabolite have assumed importance.

A series of mono- and di-fluorinated derivatives (**5**–**12**) of lead amine (**2**), and the 3′-chloro analog (**3**), have been reported (Fig. 1), some of which are even more potent and selective than their non-fluorinated counterparts, with sub-nanomolar *in vitro* GI_{50} values in sensitive cell lines.[9] Contrary to expectation, 2-(4-amino-3-methylphenyl)-4-fluorobenzothiazole (**5**: 4F 203) and the 6-fluoro isomer (**7**: 6F 203) display similar biphasic dose-response curves to that seen in the parent compound (**2**), suggesting generation of antagonizing *C*-hydroxy metabolites, whereas the 5-fluoro isomer (**6**: 5F 203) produces a 'conventional' dose-response relationship.[9] The absence of exportable metabolites from isomer (**6**) in the presence of sensitive cells confirms that oxidative metabolism of the parent benzothiazole (**2**) in the 6-position is essentially blocked by fluorination at the 5-position.[9]

This intriguing, and counter-intuitive, observation and the likely mechanistic linkage between metabolism, the unusual biphasic dose-response, and potency of compounds, has led to further investigations into the mechanism of the anti-tumor activity of benzothiazoles. Sensitivity of cell lines is strongly correlated to *inducible* CYP1A1 expression.[10] Recently, we have reported that compound (**2**) is a ligand for the arylhydrocarbon (AhR) receptor.[11] Following binding to the nuclear transporter (Arnt), and translocation to the nucleus, transcription of the CYP1A1 gene is initiated. As a substrate for CYP1A1, (**2**) is

† Part 23. For part 22 see Ref. 1.

DOI: 10.1039/b209067h

then converted to a reactive intermediate(s), presumably electrophilic in character, which induces the formation of several DNA adducts – but notably only in susceptible tumor types.[12] Adducts are also selectively generated from the 5-fluoro derivative (**6**)[13] and prodrug forms.[14]

Oxidation of benzothiazoles (Fig. 2) at several sites by

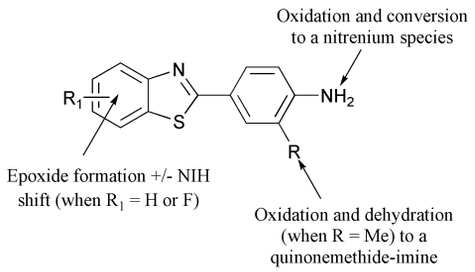

Fig. 2 Potential sites for oxidative generation of electrophilic reactive intermediates from fluorinated 2-(4-aminophenyl)benzothiazoles.

CYP1A1 could generate a range of electrophilic intermediates capable of forging covalent bonds with DNA. These sites include: (i) oxidation of the amino group to a hydroxylamine which could subsequently generate a nitrenium ion ↔ π-carbocation reactive species typically considered to be responsible for the carcinogenic/mutagenic properties of aromatic amines;[15] (ii) hydroxylation at the 3′-methyl group, followed by dehydration, would generate a quinonemethide-imine (however, this is unlikely to be a significant route in benzothiazole activation because the related 3′-halogeno agents are equiactive with the 3′-methyl series);[3] (iii) epoxidation/hydroxylation in the benzothiazole ring possibly accompanied by an NIH shift of hydride or fluoride ('fluorine walk'), or fluorine displacement,[16,17] could generate an alkylating species (*cf.* aromatic hydrocarbons).[18] Conceivably, bifunctional electrophilic agents might be generated; or, different fluoro regioisomers might generate the same reactive intermediate(s). As conventional chemical reasoning failed to explain the comparative biological responses of the fluorinated benzothiazoles, we have used frontier molecular orbital (FMO) methods to examine the metabolic activation of this beguilingly simple antitumor pharmacophore.

Results and discussion

Computational studies

The use of quantum mechanics to assess the likelihood of metabolite formation from a substrate of defined structure offers an alternative to conventional biochemical investigations. Hence we employed *ab initio* quantum mechanical calculations in an attempt to rationalize the observed differences in both the dose-response curves and metabolite formation between DF 203 (**2**) and its fluorinated analogs. Initial calibrating tests were performed using the HF/3-21G(d), HF/3-21+G(d) and HF/6-31G(d) levels of computations. The structure of 5F 203 (**6**) was optimized and compared to a previously determined X-ray crystal structure.[19] Due to the non-convergence of the HF/3-21+G(d) calculations and the time consuming nature of those performed at HF/6-31G(d) it was decided to utilize the HF/3-21G(d) level for all subsequent computations. A full potential energy surface was calculated for rotation about the benzothiazole ring–phenyl ring bond and the minimum energy structure identified. The crystal structure of **6** was reproduced with a root mean squared deviation (rmsd) of 0.007Å in the bond lengths and an rmsd of 0.95° in the bond angles. In view of this close similarity in geometries, it was not surprising that electrostatic potential (ESP) maps calculated for the crystal structure and the HF/3-21G(d) optimized geometries proved qualitatively the same. The optimized structure is planar, in agreement with the crystal geometry: the planar, aromatic nature of these compounds makes them ideal substrates for CYP1A1.[20]

FMO theory has been formulated to predict the relative reactivities of series of structurally-related molecules. Second order perturbation theory is able to divide the change in energy during a reaction into essentially steric, charge and frontier orbital contributions. When the first two terms are roughly constant the difference in reactivity can be attributed to the differences in the FMOs.[21] The highest occupied molecular orbital (HOMO) contains the electrons that are likely to be involved in a chemical reaction.

The investigation of P450 hydroxylation of medium sized molecules with FMO theory is not without precedent[22] and the regioselectivity of P450 hydroxylation has been quantitatively explained for a series of fluorobenzenes.[23] With small molecules, constraints imposed by the size and shape of the hydrophobic pocket of the P450 are not major factors in determining metabolism. As molecular size increases, accessibility to the site of metabolism becomes ever more important. Nevertheless, examinations with sterically more complicated compounds produced qualitative if not quantitative successes.[18,24] The products resulting from epoxide intermediates cannot be predicted by FMO theory as upon formation of epoxide, the site of attack does not need to be the site of hydroxylation.[18]

Benzothiazole (**2**), the monofluoro analogues (**6** and **7**) and the difluoro-benzothiazole (**9**) were initially compared on the basis of the following descriptors: the Mulliken charges,[25] the ESP, first ionization potentials (not corrected for temperature effects or zero-point energies), and the atomic contributions to FMOs.[26] No single descriptor, or combination of descriptors, correlated with observed absence of metabolism when 5F 203 (**6**) was incubated with sensitive tumor cells.[9] Electron distributions of the HOMOs of 2-(4-amino-3-methylphenyl)benzothiazole (**2**), and its 5-fluoro- and 6-fluoro-benzothiazole analogues (**6**, **7**) were very similar (Fig. 3). Comparable results were obtained for the 4-fluoro- (**5**) and 7-fluorobenzothiazoles (**8**) (data not shown). According to these calculations, there is no apparent theoretical difference in the 6 position in all five substrates (**2**, **5**–**8**) whereas experimentally *C*-6 hydroxylation is known not to occur in the 5-fluorinated compound (**6**).[9]

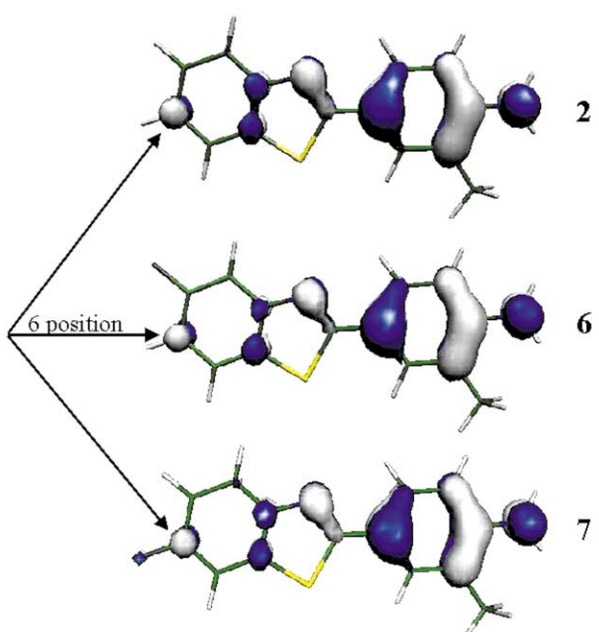

Fig. 3 Electron distribution of the HOMO of compounds 2-(4-amino-3-methyl-phenyl)benzothiazole (**2**), 2-(4-amino-3-methyl-phenyl)-5-fluorobenzothiazole (**6**) and 2-(4-amino-3-methylphenyl)-6-fluorobenzothiazole (**7**). The similarity at the 6 position is highlighted.

Subsequent investigations focused on the structures of possible reactive intermediates that could be generated after oxidation of **6** by CYP1A1. Of the several radical and cationic species examined, only the nitrenium ion ↔ π-carbocation reactive species (see Fig. 4 for resonance forms) satisfactorily explains the distinction between **6** and the other compounds. The nitrenium ion alone (Fig. 5) shows no contribution to the

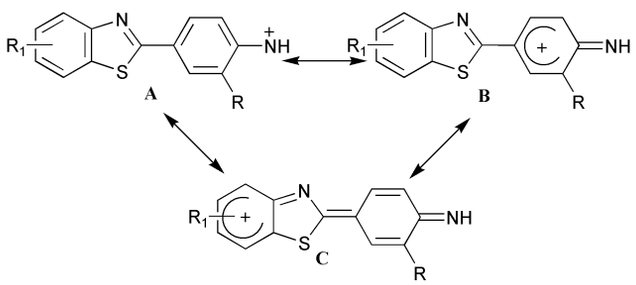

2n: R = Me, R_1 = H
3n: R = Cl, R_1 = H
5n: R = Me, R_1 = 4-F
6n: R = Me, R_1 = 5-F
7n: R = Me, R_1 = 6-F
8n: R = Me, R_1 = 7-F
9n: R = Me, R_1 = 5,6-di-F
10n: R = Me, R_1 = 4,5-di-F
11n: R = Me, R_1 = 5,7-di-F
12n: R = Cl, R_1 = 5-F

Fig. 4 Structures of **n**itrenium ions ('**n**' series) with positive charge localized on the exocyclic nitrogen atom (A) and delocalized π-carbocation resonance forms (B, C).

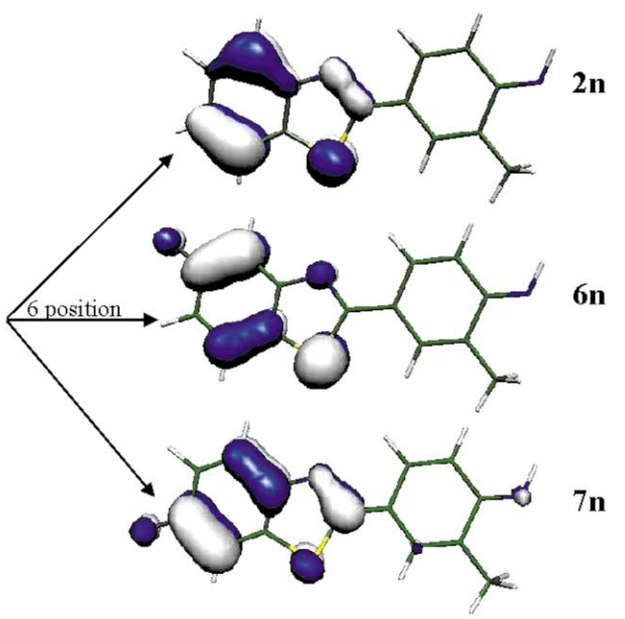

Fig. 5 Electron distribution of the HOMO of the nitrenium ion intermediates (**2n**), (**6n**) and (**7n**). The differences at the 6-position are highlighted.

HOMO in the 6 position for the 5-fluoro species (**6n**) whereas there is significant electron population at this position for reactive intermediates (**2n**) and (**7n**). Therefore the HOMO of the nitrenium ion intermediates display features that correlate with experimental observations, notably the differences seen in the dose-response curve and detection of exportable metabolite. In order to validate these results the HOMO distributions of compounds (**2n**, **6n** and **7n**) were recomputed at the correlated MP2/6-31G(d) level of theory and revealed the same characteristics as the lower level calculations.

Wave functions were then generated for two more nitrenium ions (**3n** and **12n**) derived from amines (**3** and **12**) which had been synthesized previously but not previously subjected to

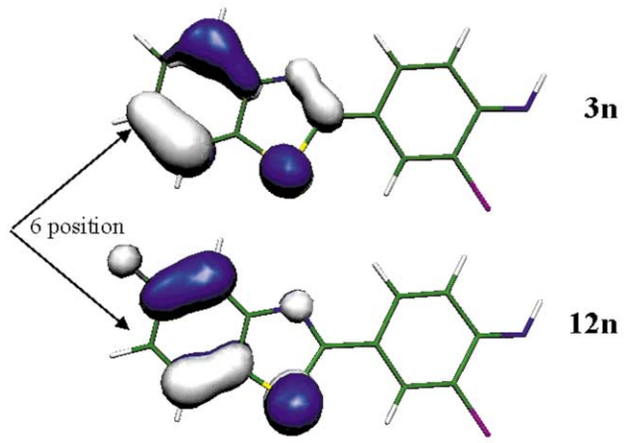

Fig. 6 Electron distribution of the HOMO of the nitrenium ion intermediates (**3n**) and (**12n**). The presence or absence of electron density at the 6-position is highlighted.

metabolic analysis.[9] The HOMO distributions of these reactive intermediates (**3n**, **12n**), respectively, can be seen in Fig. 6. In a pattern identical to the corresponding 3′-methyl compounds, 2-(4-amino-3-chlorophenyl)benzothiazole (**3**) was predicted to form a bioactive nitrenium ion ↔ π-carbocation reactive intermediate (**3n**) which would be inactivated by 6-hydroxylation whereas this would not occur with the fluorinated counterpart (**12n**). Similarly, HOMO distributions of difluorobenzothiazoles (**10** and **11**) and their derived nitrenes (**10n** and **11n**) suggested that neither should undergo hydroxylation at *C*-6 (data not shown).

As predicted by *ab initio* FMO calculations, the difluorobenzothiazoles (**10**, **11**) and 2-(4-amino-3-chlorophenyl)-5-fluorobenzothiazole (**12**) produced no exportable metabolites *in vitro* when incubated for > 7 d in the presence of human breast MCF-7 cells (data not shown). In contrast, polar biotransformation products were exported into nutrient media 24 h after treatment of cells by the parent amines (**2**) and (**3**). Differences in the metabolism/bioactivation pathways of **3** and **12** are echoed in their dose-response profiles against MCF-7 cells *in vitro*. Compound (**3**) showed a biphasic relationship (*cf.* **2**)[3] with a second growth phase at 1–100 μM (Fig. 7)

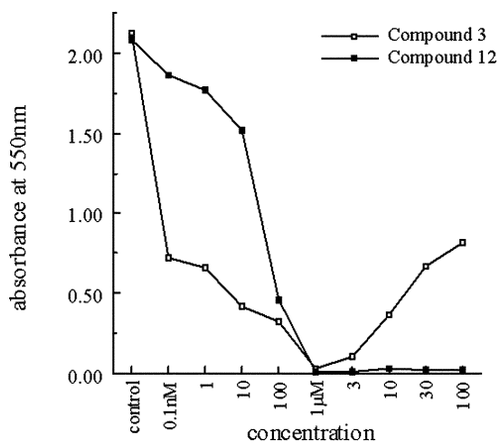

Fig. 7 Dose-response curves of 2-(4-amino-3-chlorophenyl)benzothiazole (**3**) and 2-(4-amino-3-chlorophenyl)-5-fluorobenzothiazole (**12**) against MCF-7 cells *in vitro*.

whereas the 5-fluoro-benzothiazole (**12**) shows a conventional dose-response relationship without a second growth phase (*cf.* **6**).

A possible scenario for the bioactivation of antitumor 2-(4-aminophenyl)benzothiazoles is proposed and exemplified by the metabolism of 2-(4-amino-3-methylphenyl)benzothiazole (**2**) (Scheme 1). CYP1A1-mediated transformation,

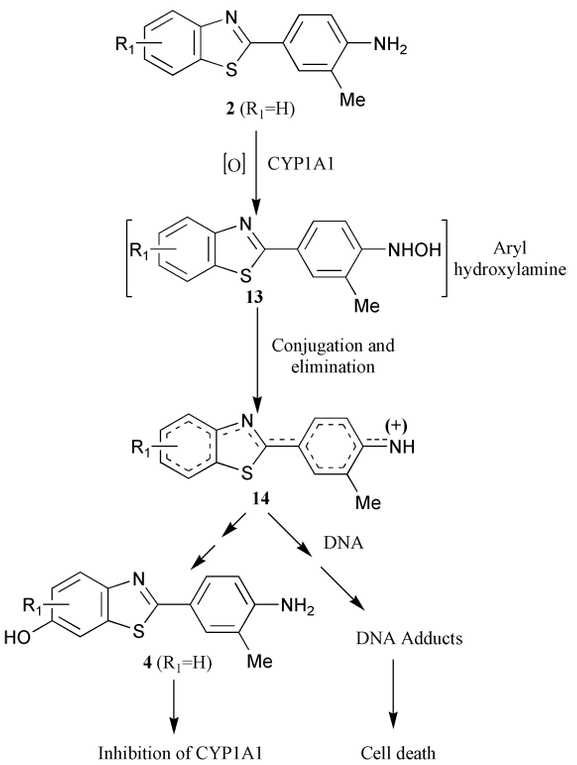

Scheme 1 Putative bioactivation pathway for 2-(4-amino-3-methylphenyl)benzothiazole (**2**).

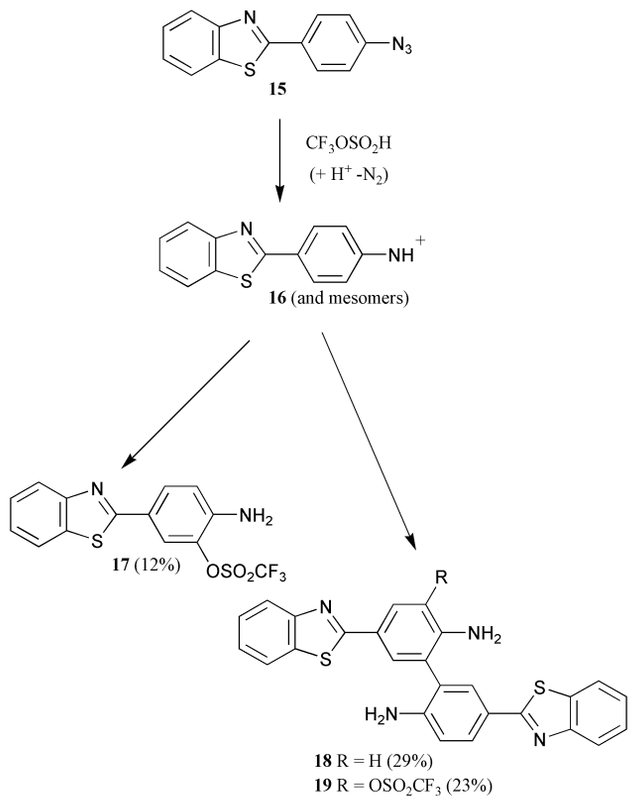

Scheme 2 Intermolecular trapping of the nitrenium species generated from 2-(4-azidophenyl)benzothiazole (**16**).

probably *via* an aryl hydroxylamine intermediate (**13**), followed by conjugation (as a sulfate or glucuronide) and elimination, would generate a nitrenium ↔ π-carbocation reactive species (see **14** which depicts a concensus mesomeric structure).

In compounds that produce an exportable metabolite, there may be the formation of a 6-hydroxy metabolite that reversibly inhibits the P450.[8] This process accounts for the unusual biphasic dose-response relationship against sensitive cell lines observed *in vitro* (*e.g.* with compounds **2**, and also **3**, **5** and **7**). We cannot exclude the possibility that (**2**) may undergo direct oxidation (CYP1A1) at the 6-position and that the 6-hydroxy metabolites may then be a substrate for further metabolism.

In all the benzothiazoles, but more prominently in those cases where 6-hydroxylation is disfavoured (*e.g.* **6**, **9**, **12**), the reactive intermediate may form damaging DNA adducts in sensitive cell types which then engage apoptotic signalling events. Appropriate gene expression changes corroborating these events in sensitive MCF-7 cells have been tracked using cDNA microarrays but, significantly, no such gene expression changes have been observed in insensitive breast MDA-MB-435.[27]

We have adduced evidence for this proposal from our earlier work on the decomposition of 2-(4-azidophenyl)benzothiazoles.[28] When azide (**15**) was decomposed in triflic acid at 0 °C the nitrene intermediate formed (**16**) underwent competing reactions: either quenching with triflic acid to afford the triflate (**17**); or intermolecular coupling to yield two biphenyls (**18**, **19**) (Scheme 2)). Under these experimental conditions of high concentration, possibly involving intimate ion-pairing within a solvent cage, adduct formation from the nitrenium species (**16**) occurs at the 2-phenyl residue rather that at the benzothiazole moiety. It is a moot point as to where conjugation between reactive intermediates generated from antitumor benzothiazoles and DNA under physiological conditions may occur.

Conclusion

Frontier molecular orbital analysis of antitumor 2-(4-aminophenyl)benzothiazoles can rationalize the propensity of their CYP1A1-generated reactive intermediates to undergo deactivating *C*-hydroxylation, or to bind covalently to DNA. Examples of the former substrates are 2-(4-amino-3-methylphenyl)benzothiazole (**2**), 2-(4-amino-3-chlorophenyl)-benzothiazole (**3**) and 2-(4-amino-3-methylphenyl)-6-fluorobenzothiazole (**7**): examples of the latter, where chemical reactivity is specifically sequestered within DNA of susceptible cells, are 2-(4-amino-3-methylphenyl)-5-fluorobenzothiazole (**6**: 5F 203) and 2-(4-amino-3-chlorophenyl)-5-fluorobenzothiazole (**12**).

This work points to activation of the amino group of active benzothiazoles along the nitrenium ion ↔ π-carbocation pathway, and suggests that DNA adducts derived from epoxide intermediates (see Fig. 2) are unlikely. In formulating this conclusion it is important to note that the *in vitro* antitumor profiles of the active 2-(4-aminophenyl)benzothiazoles are starkly different from those of carcinogenic amines and polycyclic hydrocarbons which also induce, and are metabolized by, CYP1A1. We are currently conducting studies to elucidate the structures of the DNA adducts formed by these enigmatic benzothiazoles, and to determine why they are so damaging to tumor cells. The L-lysylamide (dihydrochloride) prodrug form of 5F 203 ('Phortress')[14] has been selected for clinical trials by the Cancer Research UK.

Experimental section

Computational details

All the quantum mechanical calculations were carried out on a Silicon Graphics Origin 200 running the IRIX 6.5 operating system, using Gaussian98.[29] Molecular orbital visualization and the production of the orbital plots has been done using the freely available Molekel program.[30,31]

Growth inhibitory assays

Benzothiazole analogs were prepared as 10 mM top stocks, dissolved in DMSO, and stored at 4 °C, protected from light for a maximum period of 4 weeks. MCF-7 (ER+) and MDA 468

(ER−) human derived breast carcinoma cells, cultivated at 37 °C in an atmosphere of 5% CO_2 in RPMI 1640 medium supplemented with 2 mM L-glutamine and 10% fetal calf serum (FCS) were routinely subcultured twice weekly to maintain in continuous logarithmic growth. Cells were seeded into 96-well microtiter plates at a density of 5×10^3 per well and allowed 24 h to adhere before drugs were introduced (final concentration 0.1 nM–100 μM, $n = 8$). Serial drug dilutions were prepared in medium immediately prior to each assay. At the time of drug addition and following 72 h exposure, MTT was added to each well (final concentration 400 μg mL^{-1}). Incubation at 37 °C for 4 h allowed reduction of MTT by mitochondrial dehydrogenase to an insoluble formazan product. Well contents were aspirated and formazan solubilized by addition of DMSO:glycine buffer (pH 10.5) (4:1). Absorbance was read on an Anthos Labtec systems plate reader at 550 nm as a measure of cell viability; thus cell growth or drug toxicity was determined.

References

1 C.-O. Leong, M. Gaskell, E. A. Martin, R. T. Heydon, P. B. Farmer, M. C. Bibby, P. A. Cooper, J. A. Double, T. D. Bradshaw and M. F. G. Stevens, *Br. J. Cancer*, in press.
2 M. F. G. Stevens, C. J. McCall, P. Lelieveld, P. Alexander, A. Richter and D. E. Davies, *J. Med. Chem.*, 1994, **37**, 1689–1695.
3 D.-F. Shi, T. D. Bradshaw, S. Wrigley, C. J. McCall, P. Lelieveld, I. Fichtner and M. F. G. Stevens, *J. Med. Chem.*, 1996, **39**, 3375–3384.
4 J. N. Weinstein, T. G. Myers, P. M. O'Connor, S. H. Friend, A. J. Fornace, K. W. Kohn, T. Fojo, S. E. Bates, L. V. Rubinstein, N. L. Anderson, J. K. Buolamwini, W. W. van Osdol, A. P. Monks, D. A. Scudiero, E. A. Sausville, D. W. Zaharevitz, B. Bunow, V. N. Viswanadhan, G. S. Johnson, R. E. Wittes and K. D. Paull, *Science*, 1997, **275**, 343–349.
5 T. D. Bradshaw, D.-F. Shi, R. J. Schultz, K. D. Paull, L. Kelland, A. Wilson, H. H. Fiebig, S. Wrigley and M. F. G. Stevens, *Br. J. Cancer*, 1998, **78**, 421–429.
6 T. D. Bradshaw, S. Wrigley, D.-F. Shi, R. J. Schultz, K. D. Paull and M. F. G. Stevens, *Br. J. Cancer*, 1998, **77**, 745–752.
7 E. Kashiyama, I. Hutchinson, M.-S. Chua, S. F. Stinson, L. R. Phillips, G. Kaur, E. A. Sausville, T. D. Bradshaw, A. D. Westwell and M. F. G. Stevens, *J. Med. Chem.*, 1999, **42**, 4172–4184.
8 M.-S. Chua, E. Kashiyama, T. D. Bradshaw, S. F. Stinson, E. Brantley, E. A. Sausville and M. F. G. Stevens, *Cancer Res.*, 2000, **60**, 5196–5203.
9 I. Hutchinson, M.-S. Chua, H. L. Browne, V. Trapani, T. D. Bradshaw, A. D. Westwell and M. F. G. Stevens, *J. Med. Chem.*, 2001, **44**, 1446–1455.
10 C. Hose, M. Rivera, E. A. Sausville and A. Monks, *Proc. Am. Assoc. Cancer Res.*, 2001, **42**, 2749.
11 A. I. Loaiza-Pérez, V. Trapani, C. Hose, S. S. Singh, J. B. Trepel, M. F. G. Stevens, T. D. Bradshaw and E. A. Sausville, *Mol. Pharmacol.*, 2002, **61**, 13–19.
12 M. F. G. Stevens, R. T. Heydon, E. A. Martin, P. B. Farmer, T. D. Bradshaw, I. Hutchinson, A. D. Westwell, H. L. Browne and V. Trapani, *Proc. Am. Assoc. Cancer Res.*, 2001, **42**, 1754.
13 T. D. Bradshaw, C.-O. Leong, M. Gaskell, P. B. Farmer, M. C. Bibby, J. A. Double, P. A. Cooper, E. A. Sauseville and M. F. G Stevens, *Proc. Am. Assoc. Cancer Res.*, 2002, **43**, 4757.
14 I. Hutchinson, S. A. Jennings, B. R. Vishnuvajjala, A. D. Westwell and M. F. G. Stevens, *J. Med. Chem.*, 2002, **45**, 744–747.
15 E. K. Weisburger, in *Carcinogenesis*, ed. M. P. Waalkes and J. M. Ward, Raven Press, New York, 1994, pp. 9–11.
16 G. J. Dear, I. M. Ismail, P. J. Mutch, R. S. Plumb, L. H. Davies and B. C. Sweatman, *Xenobiotica*, 2000, **30**, 407–426.
17 J. Koerts, A. E. M. F. Soffers, J. Vervoort, A. De Jager and I. M. C. M. Rietjens, *Chem. Res. Toxicol.*, 1998, **11**, 503–512.
18 J. Koerts, M. M. C. Velraeds, A. E. M. F. Soffers, J. Vervoort and I. M. C. M. Rietjens, *Chem. Res. Toxicol.*, 1997, **10**, 279–288.
19 C. H. Schwalbe, personal communication.
20 D. F. V. Lewis, *Toxicol. Model.*, 1995, **1**, 8–97.
21 I. Fleming, *Frontier Orbitals and Organic Chemical Reactions*, Wiley Redwood Books, Trowbridge, Wiltshire, 1976, pp. 1–10.
22 B. Kuhn, W. Jacobsen, U. Christians, L. Z. Benet and P. A. Kollman, *J. Med. Chem.*, 2001, **44**, 2027–2034.
23 I. M. C. M. Rietjens, A. E. M. F. Soffers, C. Veeger and J. Vervoort, *Biochemistry*, 1993, **32**, 4801–4812.
24 D. F. V. Lewis, B. G. Lake, S. G. George, M. Dickins, P. J. Eddershaw, M. H. Tarbit, A. P. Beresford, P. S. Goldfarb and F. P. Guengerich, *Toxicology*, 1999, **139**, 53–79.
25 R. S. Mulliken, *J. Chem. Phys.*, 1955, **23**, 1833–1840.
26 K. Fukui, T. Yonezawa, C. Nagata and H. Shingu, *J. Chem. Phys.*, 1954, **22**, 1433–1442.
27 A. Monks, M. I. Rivera, E. Harris, C. Hose and E. A. Sausville, *Proc. Am. Assoc. Cancer Res.*, 2001, **42**, 3417.
28 M. F. G. Stevens, D.-F. Shi and A. Castro, *J. Chem. Soc., Perkin Trans. 1*, 1995, 83–93.
29 GAUSSIAN98 Gaussian 98, Revision A.7. M. J. Frisch, G. W. Trucks, H. B. Schlegel, G. E. Scuseria, M. A. Robb, J. R. Cheeseman, V. G. Zakrzewski, J. A. Montgomery, R. E. Stratmann, J. C. Burant, S. Dapprich, J. M. Millam, A. D. Daniels, K. N. Kudin, M. C. Strain, O. Farkas, J. Tomasi, V. Barone, M. Cossi, R. Cammi, B. Mennucci, C. Pomelli, C. Adamo, S. Clifford, J. Ochterski, G. A. Petersson, P. Y. Ayala, Q. Cui, K. Morokuma, D. K. Malick, A. D. Rabuck, K. Raghavachari, J. B. Foresman, J. Cioslowski, J. V. Ortiz, A. G. Baboul, B. B. Stefanov, G. Liu, A. Liashenko, P. Piskorz, I. Komaromi, R. Gomperts, R. L. Martin, D. J. Fox, T. Keith, M. A. Al-Laham, C. Y. Peng, A. Nanayakkara, C. Gonzalez, M. Challacombe, P. M. W. Gill, B. Johnson, W. Chen, M. W. Wong, J. L. Andres, C. Gonzalez, M. Head-Gordon, E. S. Replogle, J. A. Pople, Gaussian, Inc., Pittsburgh PA, 1998.
30 P. F. Flükiger, PhD Thèse No 2561, Département de chimie physique, Université de Genève, Genève, 1992.
31 S. Portmann and H. P. Lüthi, *Chimia*, 2000, **54**, 766–770.